A VEGFR2 Antagonist Inhibits Cell Proliferation, Migration, and Invasion by Blocking the PI3K-Akt and MAPK Signaling Pathways in Thyroid Cancer

Chunhao Liu
Peking Union Medical College Hospital
Zhao Liu
Xi'an Jiaotong University
Hao Zhao
Peking Union Medical College Hospital
Yue Cao
Peking Union Medical College Hospital
Yansong Lin
Peking Union Medical College Hospital
Xiaoyi Li (li.xiaoyi@263.net)
Peking Union Medical College Hospital https://orcid.org/0000-0003-2612-0871

Research Article

Keywords: VEGFR2, Apatinib, Thyroid cancer

Posted Date: June 22nd, 2021

DOI: https://doi.org/10.21203/rs.3.rs-625662/v1

Abstract

Background: Vascular endothelial growth factor receptor-2 (VEGFR2)-mediated signaling cascades are involved in proliferation, migration, survival, and permeability changes in vascular endothelial cells. It was thought that VEGFR2 antagonists exerted their antitumor effects by inhibiting angiogenesis in tumor tissues. However, some recent studies have found that they have significant direct antitumor effects in some tumors. The aim of this study was to explore the antitumor effects and mechanisms of VEGFR2 antagonists in thyroid cancer (TC).

Methods: The antitumor efficacy of a VEGFR2 antagonist (apatinib) in TC cells was evaluated through a series of in vitro experiments, and xenograft models were used to test its in vivo antitumor activity. The antitumor mechanisms of the VEGFR2 antagonist were explored using western blotting and immunohistochemistry.

Results: Compared with that in the normal human thyroid cell line HTori3, the expression of VEGFR2 in TC cell lines (including IHH4, BCPAP, TPC-1, C643, K1, and 8305C) was significantly increased, especially in the C643 and 8305C cell lines. VEGFR2 antagonist inhibited the proliferation of C643 and 8305C cells in a dose-dependent manner, significantly reduced the invasion and migration of these cells, induced G0/G1 phase arrest and promoted cancer cell apoptosis. Additionally, the antiproliferative effect of the VEGFR2 antagonist was significantly reduced after KDR gene knockdown. In vivo experiments showed that tumor growth in nude mice was significantly inhibited in response to apatinib. The western blot and immunohistochemistry results showed that the VEGFR2 antagonist significantly reduced the expression and phosphorylation of VEGFR2 and further inhibited the phosphorylation of the downstream molecules Akt and ERK1/2.

Conclusions: The VEGFR2 antagonist inhibited cell proliferation, invasion and migration in TC by inhibiting the PI3K/Akt and MAPK signaling pathways and exerted direct antitumor effects. Thus, directly targeting VEGFR2 can be an effective strategy for TC expressing VEGFR2.

Introduction

Thyroid cancer (TC) is the most common endocrine malignancy, accounting for 3.1% of all cancers. The global incidence of TC in 2018 was 6.7%, with approximately 560,000 new cases worldwide [1, 2]. Approximately 96% of TCs originate from thyroid follicular cells, and approximately 98% of cases are differentiated thyroid cancers (DTCs) [3]. Due to the indolent course of DTCs and establishment of standard management strategies, most patients can live for a long time without recurrence and metastasis. However, it has been reported that 6–13% of patients have lesions that invade critical surrounding structures [4–6]; in addition, 5.9–23% of patients have distant metastasis, and 2.2–9% of these patients are diagnosed with distant metastasis at presentation [6–8]. In locally advanced patients, the 5-year disease-specific survival (DSS) rate is only 67.9% for patients who have gross residual disease after surgery[9], and patients with distant metastasis have a worse 10-year DSS rate, only approximately

26–70% [10, 11]. Although anaplastic thyroid carcinoma accounts for only 2% of TCs, it is responsible for 40–50% of TC-related deaths [12]. For patients with anaplastic thyroid carcinoma, regular treatment strategies have limited effects, but targeted therapy may offer new hope.

Vascular endothelial growth factor (VEGF) is regarded as a key proangiogenic factor that drives tumor angiogenesis to promote solid tumor growth [13]. VEGF regulates endothelial cell function by binding to three membrane receptor tyrosine kinases (RTKs): vascular endothelial growth factor receptor-1 (VEGFR1, Flt1), vascular endothelial growth factor receptor-2 (VEGFR2, KDR) and vascular endothelial growth factor receptor-3 (VEGFR3, Flt4). Among these receptors, VEGFR2 plays an essential role in mediating the mitogenic, angiogenic, and permeability-enhancing effects of VEGF [14]. Inhibiting angiogenesis by blocking the VEGF/VEGFR2 signaling pathway has become a potential method for inhibiting tumor growth [15–17]. Recently, the U.S. The Food and Drug Administration (FDA) has approved two multitarget tyrosine kinase inhibitors (TKIs), sorafenib and lenvatinib, for the treatment of patients with radioactive iodine-refractory differentiated thyroid cancer (RAIR-DTC). Sorafenib and lenvatinib can prolong the progression-free survival of RAIR-DTC patients, with objective response rates (ORRs) of 12.2% and 64.8%, respectively [18, 19]. Sorafenib is a multitarget TKI that can act on VEGFR2 (IC50 = 90 nM). Lenvatinib shows more specific inhibition of VEGFR2 (IC50 = 4 nM) and also inhibits VEGFR3. Lenvatinib has better treatment efficacy than sorafenib [20]. that the success of these drugs suggests that VEGFRs, especially VEGFR2, are an essential therapeutic target in TC.

Apatinib (YN968D1) is a novel and highly selective inhibitor of the VEGFR2 tyrosine kinase with a binding affinity 90 times greater than that of sorafenib [21–22]. In several phase II clinical trials, apatinib has shown promising therapeutic effects against diverse tumor types [23–27], especially TC [28]. Recent studies have shown that apatinib can directly inhibit the growth of tumor cells that express VEGFR2 [29–32]. However, the effect of apatinib on TC cells and its underlying antitumor mechanisms are rarely reported. This study was designed to evaluate the effects of apatinib on TC cell lines both in vivo and in vitro, as well as to investigate the possible direct antitumor mechanisms.

Material And Methods

Human thyroid cancer cell lines and drug treatments

Dr Peng Hou (The First Affiliated Hospital of Xi’an Jiaotong University College of Medicine, Xi’an, China) provided the human TC cell lines TPC-1, K1, BCPAP, IHH4, 8305C, and C643 and the normal thyroid cell line HTori3. All cell lines used in this study were authenticated by short tandem repeat analysis at Genesky Co., Ltd., and the results were confirmed by Professor Hou Peng's group [33]. The cells were routinely cultured at 37°C in RPMI 1640 with 10% fetal bovine serum. In some experiments, cells were treated with apatinib at the indicated concentrations and for the indicated times, and the medium and agent were replenished every 24 h (Jiangsu Hengrui Medicine Co., Ltd, Jiangsu, China). The drugs were dissolved in dimethyl sulfoxide (DMSO), aliquoted, and stored at -80°C until use. The same volume of DMSO was used as a vehicle control.

Cell proliferation assay

Cells (1*103/well) were seeded in 96-well plates and cultured with various concentrations of apatinib for 96 h. The MTT assay was then performed to evaluate cell proliferation, as previously described. Six triplicates were performed to determine each data point.

After reaching a confluence of 50–60%, 8305C and C643 cells were infected with retroviral particles carrying sh-KDR hairpin sequences. In short, the culture medium was replaced by an infection mix containing 0.5 mL of complete medium, 0.5 mL of retrovirus-containing medium, and 5 μL of polybrene (Sigma Aldrich, San Luis, MO, USA). After further incubation for 24 h at 37 ◦C and 5% CO2, the infection mix was removed and replaced by fresh complete medium. After 48 h, the knockdown efficiency was evaluated by western blot analyses. The MTT assay was then performed to evaluate the proliferation of sh-KDR cells. Six triplicates were performed to determine each data point.

Colony formation assay

Cells were seeded in 12-well plates at a density of 6,000-8,000 cells/mL and treated with the indicated concentration of apatinib or DMSO for 10-14 days. Cells were then fixed with methanol and stained with crystal violet.

Transwell assay

Cells (1*105) were seeded into noncoated upper chambers of transwell plates (8 mm pore size; Corning) for migration assays and into Matrigel-coated upper chambers (BD Bioscience, 354234) for invasion assays with or without apatinib. After culture for 24 h, cells were fixed with methanol and stained with a 0.1% crystal violet solution. Migrated cell populations were evaluated in five fields per well under a microscope.

Apoptosis and cell cycle assays

For apoptosis assays, cells were treated with apatinib or DMSO for 48 h, harvested, washed with phosphate-buffered saline (PBS), and stained with the Annexin V-FLUOS Staining Kit (Roche Applied Science, Penzberg, Germany) according to the manufacturer's protocol. Apoptotic cells were analyzed by a flow cytometer. Each experiment was performed in triplicate. For the cell cycle assay, 8305C and C643 cells in the logarithmic growth phase were serum starved for 12 h and treated with apatinib or DMSO for the indicated time. Next, cells were harvested and fixed in ice-cold 70% ethanol for at least 30 min. After washing twice with PBS, propidium iodide (PI) solution (50 μg/mL PI, 50 μg/mL RNase A, 0.1% Triton-X, and 0.1 mM EDTA) was added to stain the cells. Cells were then subjected to flow cytometry analysis to determine cell cycle distributions.

Western blot analysis

The indicated cells (5 × 105/well) were seeded in 6-well plates and cultured in RPMI 1640 medium containing 10% FBS. Then, the cells were treated with apatinib or DMSO for the indicated times. Finally, cells were lysed, and the lysates were subjected to sodium dodecyl sulfate-polyacrylamide gel electrophoresis (SDS-PAGE) analysis. After being blocked with 5% bovine serum albumin (BSA) in Tris-buffered saline with Tween 20 (TBST; 120 mM Tris–HCl (pH 7.4), 150 mM NaCl, and 0.05% Tween 20) for 1 h at room temperature, the membranes were incubated with specific primary antibodies overnight at 4°C. Antibodies against the following molecules were used in this study: phospho-VEGFR2 (ab38473, Abcam), FLK-1 (sc-47778, Santa Cruz Biotechnology), phospho-Akt (BS4007, Bioworld Technology), Akt (BS1810, Bioworld Technology), phospho-ERK (#4370, CST), ERK (#4695, CST), ERK (BS6426, Bioworld Technology), Bcl-2 (sc-7382, Santa Cruz Biotechnology), Bax (sc-7480, Santa Cruz Biotechnology), N-cadherin (#13116, CST), E-cadherin (#3195, CST), Slug (bs-1382R, Bioss), Snail1 (13099-1-AP, ProteinTech), MMP9 (10375-2-AP, ProteinTech), cyclin E (sc-377100, Santa Cruz Biotechnology), cyclin D1 (sc-8396, Santa Cruz Biotechnology), Cdk2 (sc-6248, Santa Cruz Biotechnology), Cdk4 (sc-23896, Santa Cruz Biotechnology), p27 (sc-1641, Santa Cruz Biotechnology), p21 (sc-6246, Santa Cruz Biotechnology), Ki-67 (550609, BD Pharmingen), GAPDH (M20006, Abmart), and β-actin (sc-47778; Santa Cruz Biotechnology). After incubation with HRP-conjugated secondary antibodies from ZSGB-BIO, immunoblot signals were analyzed by the Western Bright ECL detection system (Advansta, CA).

Tumor xenografts

Three- to four-week-old female athymic nude mice were purchased from SLAC Laboratory Animal Co., Ltd. (Shanghai, China) and housed in a specific pathogen-free environment. C643 (4 × 106) cells were injected subcutaneously into the left armpit region of nude mice. When tumors grew to approximately 5 mm in diameter, mice were randomly divided into two groups (six mice per group) and given apatinib (100 mg/kg). Drugs were dissolved and administered to mice by intraperitoneal injection for 14 consecutive days followed by 7 rest days. Tumor volumes were measured by a Vernier caliper every 3 days and calculated by the following formula: tumor volume (mm3) = l*w2*0.5, where l is the length and w is the width. Twenty-one days after apatinib administration, mice were sacrificed by cervical dislocation, and tumors were then harvested and weighed. All animal experiments were conducted and approved by the Laboratory Animal Center of Xi'an Jiaotong University (Xi'an, P.R. China).

Immunohistochemistry

After a cycle (21 days) of apatinib administration, mice were sacrificed by cervical dislocation. Tumor tissues were collected, fixed in 4% formaldehyde, and embedded in paraffin. Then, samples were cut into consecutive 4 μm sections and stored at -80°C for further analyses. Tumor tissue specimens from 3 PTC patients treated with apatinib were also collected for immunohistochemical analysis.

For immunohistochemical analysis, paraffin sections were deparaffinized in xylene and hydrated in gradient alcohol (100%, 95%, 85%, and 75%). Then, sections were incubated in 3% H2O2 to block endogenous peroxidase activity and subjected to antigen retrieval in 0.01 mol/L citrate buffer. After being washed with PBS, the sections were blocked in 1% BSA and incubated with mouse primary antibodies

directed against VEGFR2, p-VEGFR2, Ki-67, p-Akt and p-ERK at 4°C overnight (antibodies directed against VEGF and VEGFR2 were used in tumor tissue specimens from PTC patients). Then, the sections were incubated with the corresponding secondary antibodies at 37°C for 45 min. After being washed with PBS, the sections were stained with DAB and counterstained in hematoxylin. Based on the average percentage of positive cells calculated from at least 10 representative fields (x400 magnification), positive staining was defined as a positive cell percentage of 10%. Two independent pathologists conducted the immunostaining assessment without any previous knowledge of patient clinical characteristics and outcomes.

Statistical analysis

All statistical analyses were performed using SPSS 20.0 software. Data are presented as the mean ± standard deviation. Comparisons between groups were performed with independent t-tests. Association between two numeric variables were evaluated by calculating Pearson's correlation coefficient. $P < 0.05$ was considered statistically significant.

Results

Expression of VEGFR2 in tumor specimens of RAIR-DTC patients.

Immunohistochemical analysis of tumor tissue specimens from 3 RAIR-DTC patients treated with apatinib revealed moderate or weak VEGFR2 staining intensity in 2 of 3 specimens. The patients from whom these two specimens were taken showed a partial response (PR). VEGFR2 was mainly expressed in TC cells (Table 1, Fig. 1).

Thyroid cancer cell response to apatinib correlates with VEGFR2 levels

Western blot analysis showed that VEGFR2 was expressed in all TC cell lines, including TPC-1, K1, BCPAP, IHH4, 8305C and C643, and the normal thyroid cell line HTori3, while the VEGFR2 expression levels were different in each cell line (Fig. 2A). The MTT assay suggested that apatinib suppressed the proliferation of all six TC cell lines in a dose-independent manner. However, the IC50 values varied widely between the individual cell lines (Fig. 2B). The IC50 values ranged from 15.53 μmol/L (the lowest) in C643 cells to 36.31 μmol/L (the highest) in K1 cells. In addition, the highest VEGFR2 expression level was detected in C643 cells, which presented the lowest IC50 value of the 6 TC cell lines, while the lowest was found in K1 cells, which presented the highest IC50 value (Fig. 2A and 2B) among 6 TC cell lines. Pearson's correlation analysis showed that there was a linear relationship between the expression level of VEGFR2 and the IC50 value of apatinib in TC cells (Fig. 2C; $r=-0.7616$, $p = 0.0466$).

After infection with retroviral particles carrying sh-KDR hairpin sequences, the expression level of VEGFR2 was downregulated in 8305C and C643 cells, as shown in Fig. 2D. The antiproliferative effects of apatinib were significantly inhibited in the sh-KDR group compared with those in the sh-control group. The IC50 values increased from 22.39 μM to 42.53 μM in 8305C cells and from 11.32 μM to 31.14 μM in C643 cells

(Fig. 2E). Clone formation assays revealed that the proliferation ability of TC cells was significantly inhibited in a dose-dependent manner by apatinib (Fig. 2F).

Apatinib reduces the migratory and invasive capacities of thyroid cancer cells

Transwell assays showed that apatinib decreased the migratory and invasive capacities of 8305C and C643 cells (Fig. 3A). Next, the expression levels of epithelial-mesenchymal transition (EMT)-related proteins were analyzed by western blot, and the results showed that the protein expression of N-cad, Slug, snail1 and MMP-9 was inhibited significantly by apatinib, as shown in Fig. 3B.

Apatinib induces cell cycle arrest and apoptosis in thyroid cancer cells

To determine whether apatinib inhibited cell proliferation by inducing cell cycle arrest, we evaluated the cell cycle distribution of 8305C and C643 cells treated with apatinib. As shown in Fig. 4A, the cell cycle analysis showed a statistically significant increase in cells in the G0/G1 phase in both 8305C and C643 cells ($P<0.05$). The expression of cell cycle-related proteins was further analyzed by western blot, and the results showed that cyclin-E, cyclin-D1, CDK2 and CDK4 were downregulated while p21 and p27 were upregulated in both 8305C and C643 cells after treatment with apatinib (Fig. 4B).

Flow cytometry was used to analyze the apoptosis of cells treated with apatinib. The results showed that apatinib significantly increased apoptosis compared with the control treatment (Fig. 4C). Bcl2 and Bax are key indicators of apoptosis. The expression of Bcl2 was downregulated and that of Bax was upregulated after treatment with apatinib (Fig. 4D).

Effects of apatinib on the MAPK and PI3K-Akt signaling pathways in thyroid cancer cells

The MAPK and PI3K-Akt signaling pathways are involved in the regulation of tumor cell growth, so we tested the expression of related proteins to determine the effect of apatinib on them. The western blot results showed that the expression levels of p-VEGFR2, VEGFR2, p-ERK and p-Akt in 8305C and C643 cells treated with apatinib were significantly reduced (Fig. 5A and 5B), and no significant differences were identified in the total protein levels of ERK and Akt (Fig. 5A).

Apatinib inhibits tumor growth in mice with thyroid cancer xenografts

We evaluated the antitumor potential of apatinib in a TC xenograft mouse model in vivo. Apatinib inhibited tumor growth in vivo. The tumor volume in the treatment group was decreased when compared with that in the control group (Fig. 6A and 6B). In accordance with the in vitro results, immunohistochemistry showed that apatinib reduced the expression of VEGFR2, p-VEGFR2, p-Akt and p-ERK in tumors formed by C643 cells (Fig. 6C and 6D).

Discussion

Apatinib is a small-molecule VEGFR TKI that strongly binds and inhibits VEGFR2. By blocking VEGFR2 in vascular endothelial cells, apatinib can effectively inhibit tumor angiogenesis, which further inhibits tumor growth [14, 34]. However, recent studies have shown that apatinib can directly inhibit the proliferation of tumor cells expressing VEGFR2 [31, 35–38]. Our clinical trial showed that RAIR-DTC patients obtained surprising therapeutic effects from apatinib, and the results were much better than those in other tumors [28, 39, 40]. Therefore, in this study, we explored the direct antitumor effects and mechanisms of apatinib in TC.

Our results showed that VEGFR2 was mainly expressed in TC cells in tissue samples from RAIR-DTC patients with PR, suggesting that apatinib can act on TC cells directly by blocking VEGFR2. We detected the expression levels of VEGFR2 in six TC cell lines and a normal thyroid cell line by western blot, and the results showed that the VEGFR2 expression levels were different in the six TC cell lines. Apatinib dramatically inhibited cell proliferation and colony formation, and the degree of inhibition was correlated with the levels of VEGFR2. After knocking down the gene encoding VEGFR2, the antitumor effects of apatinib on TC cell lines were significantly weakened. The above results suggest that apatinib can directly inhibit the proliferation of TC cells by suppressing VEGFR2, suggesting that VEGFR2 is the major receptor responsible for such effects. In addition, we found that apatinib significantly inhibited cell migration and invasion and decreased the expression of metastatic markers, such as Slug, snail, and MMP9, in TC cell lines. These proteins are important regulators of EMT and play an important role in the migration and invasion of tumor cells [41, 42]. Our findings are consistent with previous research in cholangiocarcinoma, which found that apatinib inhibits cellular invasion and migration by suppressing EMT [43].

We further investigated the mechanisms by which apatinib inhibits TC cells by detecting cell cycle changes, cell apoptosis, and the expression of potential downstream signaling pathway proteins. The results showed that apatinib could induce cell cycle arrest at the G0/G1 phase via downregulation of cyclin E, cyclin D, CDK2 and CDK4 and upregulation of p21 and p27. The BCL-2 protein family determines the commitment of cells to apoptosis, which is essential for development, tissue homeostasis and immunity. Lack of apoptosis can promote cancer and autoimmune diseases[44]. Our results showed that apatinib could inhibit the expression of the antiapoptotic gene Bcl2 and upregulate the expression of the proapoptotic gene Bax, which in turn induced the apoptosis of TC cells.

Studies have confirmed that the MAPK and PI3K-Akt signaling pathways are involved in regulating the cell cycle and apoptosis of tumor cells [45, 46]. We further examined the effects of apatinib on the MAPK and PI3K-Akt signaling pathways, and the results showed that apatinib could significantly downregulate the levels of p-VEGFR2, p-ERK and p-Akt. Nevertheless, the total protein levels of ERK and Akt were not significantly affected. The results imply that apatinib can exert direct antitumor effects by inhibiting the phosphorylation of members of the MAPK and PI3K-Akt signaling pathways without changing the total protein levels of ERK and Akt.

In our study, we found that the levels of VEGFR2 and p-VEGFR2 decreased significantly after treatment with apatinib, and Chen found similar results in ovarian cancer [47]. These results indicate that apatinib, as a highly selective VEGFR2 antagonist, can inhibit not only VEGFR2 phosphorylation but also VEGFR2 expression. VEGFR signaling is intricately affected by multiple factors, including receptor expression levels, the availability and affinities of different ligands, the rate of receptor cellular uptake, the extent of degradation and the speed of recycling. VEGFR endocytosis and trafficking modulate the specificity as well as the duration and amplitude of the signaling output [48]. The activation of downstream MAPK/ERK signaling, which is essential for VEGFR2 effects, is dependent on the speed of the receptor's intracellular trafficking [49, 50]. We initially detected the mRNA expression of VEGFR2 but did not observe a decrease in VEGFR2 mRNA levels (data not shown), and we suspected that apatinib may decrease VEGFR2 expression through a posttranscriptional mechanism in TC. Apatinib was believed to increase the degradation of VEGFR2, affect the movement of VEGFR2 in cells, and block the tyrosine phosphorylation sites of VEGFR2, leading to decreased phosphorylation levels of downstream MAPK and PI3K-Akt signaling pathway members[51]. However, how apatinib affects the intracellular circulation of VEGFR2 and the underlying mechanism still need to be studied.

In a xenograft model of TC, apatinib significantly delayed tumor growth in mice. The tumor volumes of the apatinib group were significantly smaller than those of the control group after the 9th day, and the final tumor weights showed the same pattern. Immunohistochemical analysis of the tumor tissue showed that the expression of VEGFR2, p-VEGFR2, Ki-67, p-Akt, and p-ERK in tumor tissue was significantly downregulated, which was consistent with the in vitro experiment results. These results also showed that apatinib could inhibit tumor growth by inhibiting the MAPK and PI3K-Akt signaling pathways in vivo.

Conclusions

In conclusion, our study elucidated that apatinib can directly inhibit the proliferation, migration and invasion of TC cells by blocking the MAPK and PI3K-Akt signaling pathways, and these effects were related to the expression level of VEGFR2. Studies to determine how apatinib affects the expression of VEGFR2 and whether it also exerts an antitumor effect by inhibiting angiogenesis in TC tissue are worthy of further exploration.

Abbreviations

VEGFR2 vascular endothelial growth factor receptor-2; VEGF vascular endothelial growth factor; TC thyroid cancer; DTCs Differentiated thyroid cancers; DSS disease-specific survival; RTKs receptor tyrosine kinases; TKIs tyrosine kinase inhibitors; RAIR-DTC radioactive iodine-refractory differentiated thyroid cancer; ORRs objective response rates; PR partial response; EMT epithelial-mesenchymal transition

Declarations

Ethics approval and consent to participate

The Ethics Committee of Peking Union Medical College Hospital approved the using of cell lines in this research. And the animal experiments were performed according to the guidelines for use and care of animals approved by Peking Union Medical College Hospital. All the patients participated in this study had signed the informed consent.

Acknowledgements

We thank Mr. Yanlong Li for statistical guidance.

Funding

This work was supported by CAMS Innovation Fund for Medical Sciences (CIFMS) (Grant Number: 2016-I2M-2-006) and the Open Project Program of Key Laboratory for Tumor Precision Medicine of Shanxi Province (Grant Number. KLTPM-SX2018-A5)

Competing interests

The authors declare that they have no competing interests.

Authors' contributions

All authors were involved in the preparation of this manuscript. Chunhao Liu: Investigation, Writing-Original Draft; Zhao Liu: Investigation, Formal analysis; Hao Zhao: Investigation; Cao Yue: Resources; Peng Hou: Resources, Methodology, Yansong Lin: Writing-Review & Editing, Supervision, Funding acquisition and Xiaoyi Li: Writing-Review & Editing, Supervision, Project administration, Conceptualization.

References

1. Bray F, Ferlay J, Soerjomataram I, Siegel RL, Torre LA, Jemal A. Global cancer statistics 2018: GLOBOCAN estimates of incidence and mortality worldwide for 36 cancers in 185 countries. CA Cancer J Clin. 2018;68(6):394-424.
2. Ferlay J, Colombet M, Soerjomataram I, et al. Estimating the global cancer incidence and mortality in 2018: GLOBOCAN sources and methods. Int J Cancer. 2019;144(8):1941-1953.
3. Fagin JA, Wells SA, Jr. Biologic and Clinical Perspectives on Thyroid Cancer. N Engl J Med. 2016;375(11):1054-1067.
4. Segal K, Shpitzer T, Hazan A, Bachar G, Marshak G, Popovtzer A. Invasive well-differentiated thyroid carcinoma: effect of treatment modalities on outcome. Otolaryngol Head Neck Surg. 2006;134(5):819-822.

5. Hay ID, Thompson GB, Grant CS, et al. Papillary thyroid carcinoma managed at the Mayo Clinic during six decades (1940-1999): temporal trends in initial therapy and long-term outcome in 2444 consecutively treated patients. World J Surg. 2002;26(8):879-885.
6. Falk SA, McCaffrey TV. Management of the recurrent laryngeal nerve in suspected and proven thyroid cancer. Otolaryngol Head Neck Surg. 1995;113(1):42-48.
7. Goffredo P, Sosa JA, Roman SA. Differentiated thyroid cancer presenting with distant metastases: a population analysis over two decades. World J Surg. 2013;37(7):1599-1605.
8. Lee J, Soh EY. Differentiated thyroid carcinoma presenting with distant metastasis at initial diagnosis clinical outcomes and prognostic factors. Ann Surg. 2010;251(1):114-119.
9. Durante C, Haddy N, Baudin E, et al. Long-term outcome of 444 patients with distant metastases from papillary and follicular thyroid carcinoma: benefits and limits of radioiodine therapy. J Clin Endocrinol Metab. 2006;91(8):2892-2899.
10. Huang IC, Chou FF, Liu RT, et al. Long-term outcomes of distant metastasis from differentiated thyroid carcinoma. Clin Endocrinol (Oxf). 2012;76(3):439-447.
11. Shoup M, Stojadinovic A, Nissan A, et al. Prognostic indicators of outcomes in patients with distant metastases from differentiated thyroid carcinoma. J Am Coll Surg. 2003;197(2):191-197.
12. Saini S, Tulla K, Maker AV, Burman KD, Prabhakar BS. Therapeutic advances in anaplastic thyroid cancer: a current perspective. Mol Cancer. 2018;17(1):154.
13. Goel HL, Mercurio AM. VEGF targets the tumour cell. Nat Rev Cancer. 2013;13(12):871-882.
14. Ferrara N, Gerber HP, LeCouter J. The biology of VEGF and its receptors. Nat Med. 2003;9(6):669-676.
15. Falcon BL, Chintharlapalli S, Uhlik MT, Pytowski B. Antagonist antibodies to vascular endothelial growth factor receptor 2 (VEGFR-2) as anti-angiogenic agents. Pharmacol Ther. 2016;164:204-225.
16. Rapisarda A, Melillo G. Role of the VEGF/VEGFR axis in cancer biology and therapy. Adv Cancer Res. 2012;114:237-267.
17. Peng FW, Liu DK, Zhang QW, Xu YG, Shi L. VEGFR-2 inhibitors and the therapeutic applications thereof: a patent review (2012-2016). Expert Opin Ther Pat. 2017;27(9):987-1004.
18. Schlumberger M, Tahara M, Wirth LJ, et al. Lenvatinib versus placebo in radioiodine-refractory thyroid cancer. N Engl J Med. 2015;372(7):621-630.
19. Brose MS, Nutting CM, Jarzab B, et al. Sorafenib in radioactive iodine-refractory, locally advanced or metastatic differentiated thyroid cancer: a randomised, double-blind, phase 3 trial. Lancet. 2014;384(9940):319-328.
20. Dunn L, Fagin JA. Therapy: Lenvatinib and radioiodine-refractory thyroid cancers. Nat Rev Endocrinol. 2015;11(6):325-327.
21. Wilhelm SM, Carter C, Tang L, et al. BAY 43-9006 exhibits broad spectrum oral antitumor activity and targets the RAF/MEK/ERK pathway and receptor tyrosine kinases involved in tumor progression and angiogenesis. Cancer Res. 2004;64(19):7099-7109.

22. Li J, Zhao X, Chen L, et al. Safety and pharmacokinetics of novel selective vascular endothelial growth factor receptor-2 inhibitor YN968D1 in patients with advanced malignancies. BMC Cancer. 2010;10:529.
23. Li J, Qin S, Xu J, et al. Apatinib for chemotherapy-refractory advanced metastatic gastric cancer: results from a randomized, placebo-controlled, parallel-arm, phase II trial. J Clin Oncol. 2013;31(26):3219-3225.
24. Li J, Tong X, Li H. Efficacy and safety of apatinib monotherapy in elderly patients with advanced metastatic non-small cell lung cancer. Indian J Cancer. 2020;57(1):13-17.
25. Zhang L, Chen L, Yu H. Phase II study of apatinib, a novel tyrosine kinase inhibitor targeting tumor angiogenesis, as second-line treatment for recurrent or advanced cervical cancer patients. Invest New Drugs. 2019.
26. Liao Z, Li F, Zhang C, et al. Phase II trial of VEGFR2 inhibitor apatinib for metastatic sarcoma: focus on efficacy and safety. Exp Mol Med. 2019;51(3):1-11.
27. Chen X, Qiu T, Zhu Y, et al. A Single-Arm, Phase II Study of Apatinib in Refractory Metastatic Colorectal Cancer. Oncologist. 2019;24(7):883-e407.
28. Zhang X, Wang C, Lin Y. Pilot Dose Comparison of Apatinib in Chinese Patients With Progressive Radioiodine-Refractory Differentiated Thyroid Cancer. J Clin Endocrinol Metab. 2018;103(10):3640-3646.
29. Peng H, Zhang Q, Li J, et al. Apatinib inhibits VEGF signaling and promotes apoptosis in intrahepatic cholangiocarcinoma. Oncotarget. 2016;7(13):17220-17229.
30. Yang C, Qin S. Apatinib targets both tumor and endothelial cells in hepatocellular carcinoma. Cancer Med. 2018;7(9):4570-4583.
31. Zheng B, Ren T, Huang Y, Guo W. Apatinib inhibits migration and invasion as well as PD-L1 expression in osteosarcoma by targeting STAT3. Biochem Biophys Res Commun. 2018;495(2):1695-1701.
32. Lin C, Wang S, Xie W, Zheng R, Gan Y, Chang J. Apatinib inhibits cellular invasion and migration by fusion kinase KIF5B-RET via suppressing RET/Src signaling pathway. Oncotarget. 2016;7(37):59236-59244.
33. Zhang Y, Sui F, Ma J, et al. Positive Feedback Loops Between NrCAM and Major Signaling Pathways Contribute to Thyroid Tumorigenesis. J Clin Endocrinol Metab. 2017;102(2):613-624.
34. Tian S, Quan H, Xie C, et al. YN968D1 is a novel and selective inhibitor of vascular endothelial growth factor receptor-2 tyrosine kinase with potent activity in vitro and in vivo. Cancer Sci. 2011;102(7):1374-1380.
35. Li X, Xu A, Li H, Zhang B, Cao B, Huang J. Novel role of apatinib as a multi-target RTK inhibitor in the direct suppression of hepatocellular carcinoma cells. Biochim Biophys Acta Mol Basis Dis. 2018;1864(5 Pt A):1693-1701.
36. Qiu H, Li J, Liu Q, Tang M, Wang Y. Apatinib, a novel tyrosine kinase inhibitor, suppresses tumor growth in cervical cancer and synergizes with Paclitaxel. Cell Cycle. 2018;17(10):1235-1244.

37. Liang S, Tong XZ, Fu LW. [Inhibitory effect of apatinib on HL-60 cell proliferation and its mechanism]. Nan Fang Yi Ke Da Xue Xue Bao. 2011;31(5):871-874.
38. Lu W, Ke H, Qianshan D, Zhen W, Guoan X, Honggang Y. Apatinib has anti-tumor effects and induces autophagy in colon cancer cells. Iran J Basic Med Sci. 2017;20(9):990-995.
39. Hu X, Cao J, Hu W, et al. Multicenter phase II study of apatinib in non-triple-negative metastatic breast cancer. BMC Cancer. 2014;14:820.
40. Li J, Qin S, Xu J, et al. Randomized, Double-Blind, Placebo-Controlled Phase III Trial of Apatinib in Patients With Chemotherapy-Refractory Advanced or Metastatic Adenocarcinoma of the Stomach or Gastroesophageal Junction. J Clin Oncol. 2016;34(13):1448-1454.
41. Jolly MK, Mani SA, Levine H. Hybrid epithelial/mesenchymal phenotype(s): The 'fittest' for metastasis? Biochim Biophys Acta Rev Cancer. 2018;1870(2):151-157.
42. Thiery JP, Sleeman JP. Complex networks orchestrate epithelial-mesenchymal transitions. Nat Rev Mol Cell Biol. 2006;7(2):131-142.
43. Huang M, Huang B, Li G, Zeng S. Apatinib affect VEGF-mediated cell proliferation, migration, invasion via blocking VEGFR2/RAF/MEK/ERK and PI3K-AKT pathways in cholangiocarcinoma cell. BMC Gastroenterol. 2018;18(1):169.
44. Czabotar PE, Lessene G, Strasser A, Adams JM. Control of apoptosis by the BCL-2 protein family: implications for physiology and therapy. Nat Rev Mol Cell Biol. 2014;15(1):49-63.
45. Hoxhaj G, Manning BD. The PI3K-AKT network at the interface of oncogenic signalling and cancer metabolism. Nat Rev Cancer. 2020;20(2):74-88.
46. Yue J, Lopez JM. Understanding MAPK Signaling Pathways in Apoptosis. Int J Mol Sci. 2020;21(7).
47. Chen L, Cheng X, Tu W, et al. Apatinib inhibits glycolysis by suppressing the VEGFR2/AKT1/SOX5/GLUT4 signaling pathway in ovarian cancer cells. Cell Oncol (Dordr). 2019;42(5):679-690.
48. Simons M, Gordon E, Claesson-Welsh L. Mechanisms and regulation of endothelial VEGF receptor signalling. Nat Rev Mol Cell Biol. 2016;17(10):611-625.
49. Nakayama M, Nakayama A, van Lessen M, et al. Spatial regulation of VEGF receptor endocytosis in angiogenesis. Nat Cell Biol. 2013;15(3):249-260.
50. Simons M. An inside view: VEGF receptor trafficking and signaling. Physiology (Bethesda). 2012;27(4):213-222.
51. Gampel A, Moss L, Jones MC, Brunton V, Norman JC, Mellor H. VEGF regulates the mobilization of VEGFR2/KDR from an intracellular endothelial storage compartment. Blood. 2006;108(8):2624-2631.

Table

Table 1 is not available with this version.

Figures

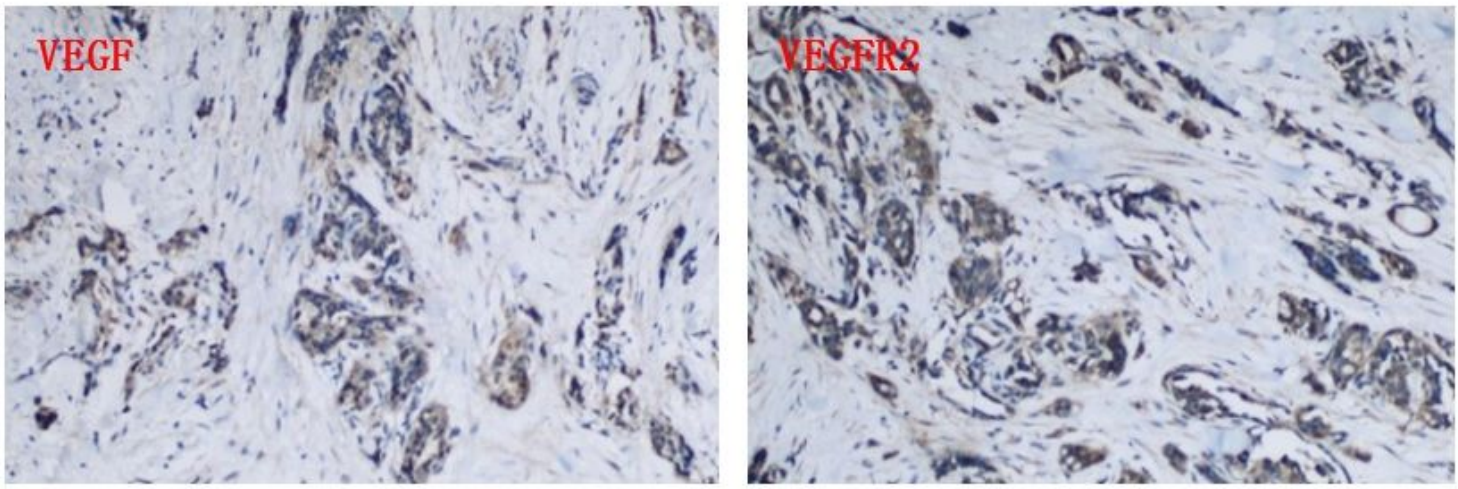

Figure 1

Representative immunohistochemical images of VEGF and VEGFR2 staining in tumor tissue specimens from PTC patients (200×).

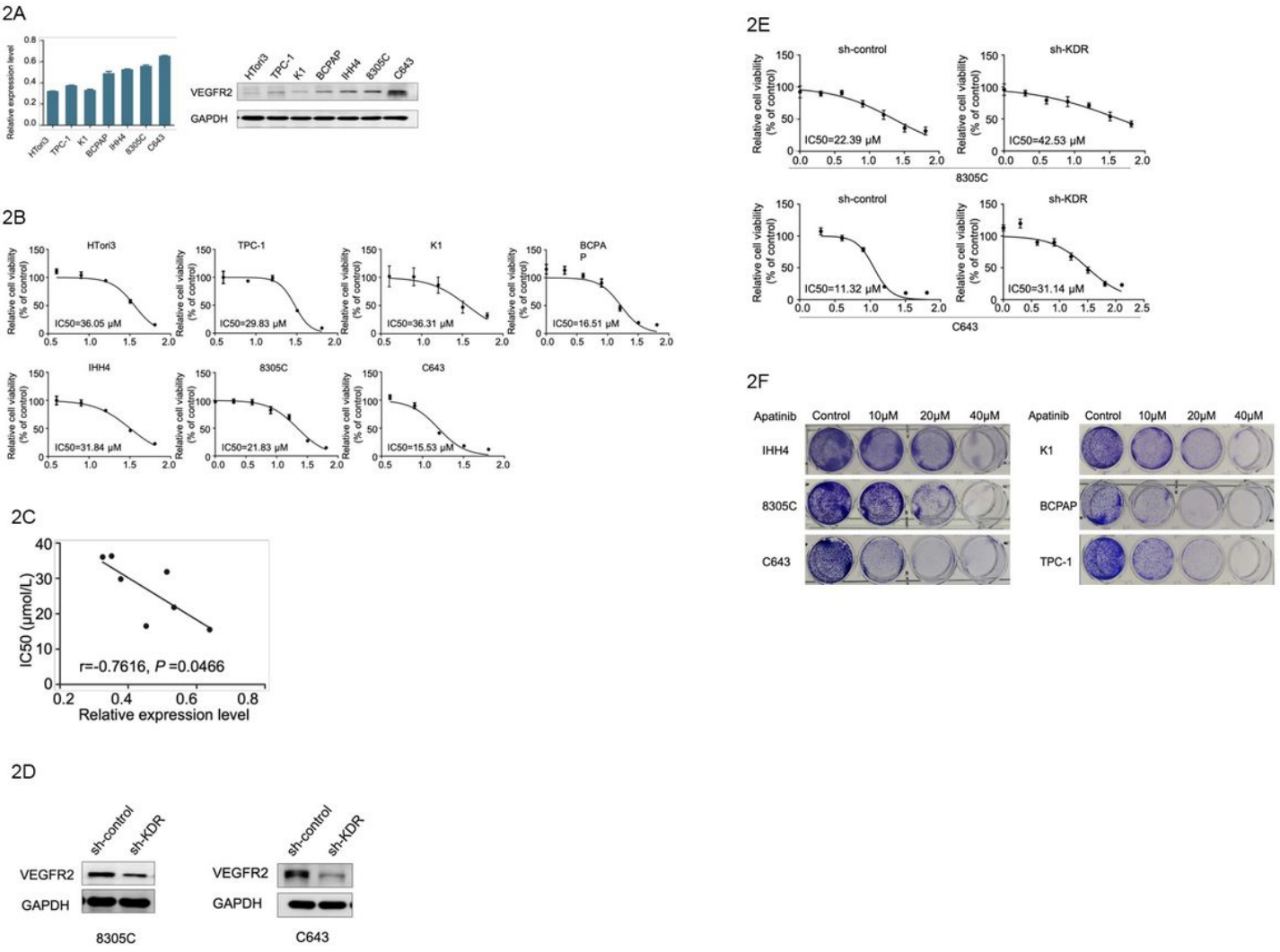

Figure 2

Apatinib-induced inhibition of TC cell proliferation is correlated with VEGFR2 expression. (a). Expression of VEGFR2 in 6 TC cell lines and one normal human thyroid cell line. (b). Cell viability and IC50 values of 6 TC cell lines and one normal human thyroid cell line. (c). Correlation between apatinib IC50 value and VEGFR2 expression level. (d). Expression of VEGFR2 in 8305C and C643 cells transfected with sh-control or sh-KDR. (e). Relative cell viability and IC50 values of 8305C and C643 cells transfected with sh-control or sh-KDR. (f). Representative images of colony formation in 6 TC cell lines.

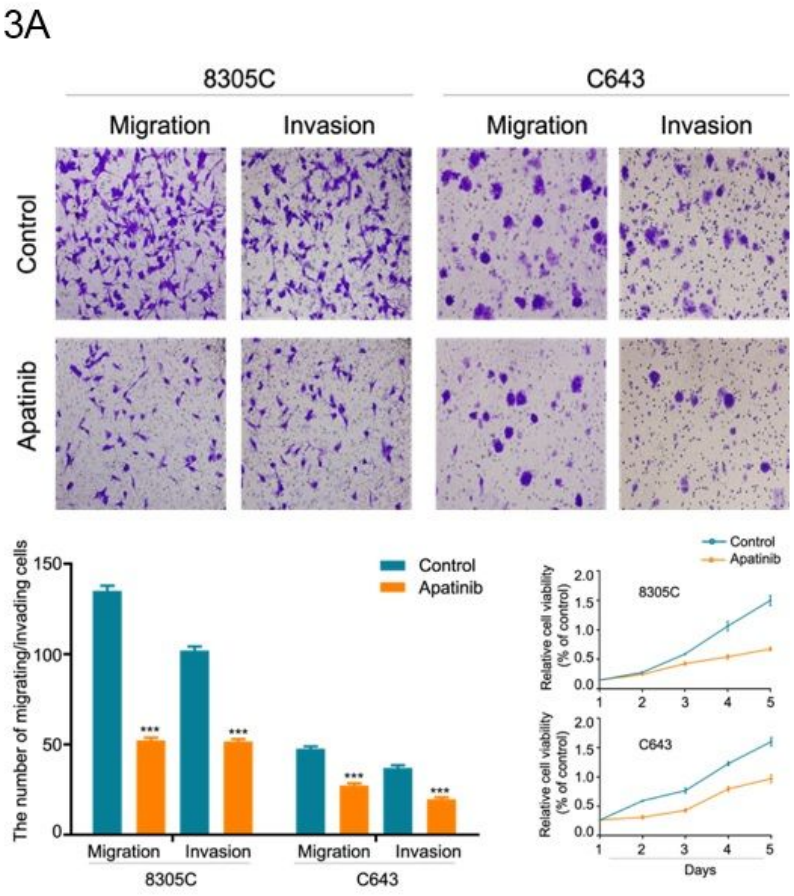

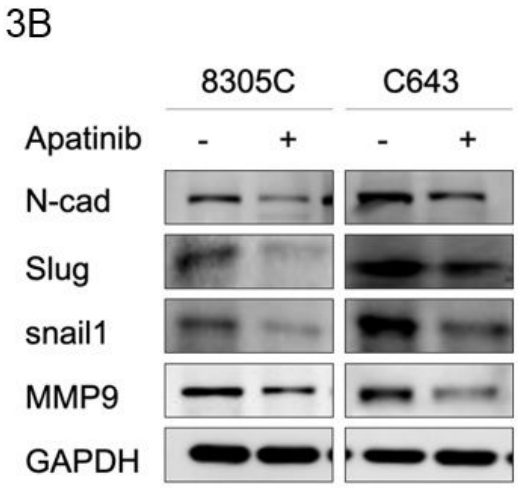

Figure 3

Apatinib reduced the migration and invasion of 8305C and C643 cells. (a). Representative images of migrating/invading 8305C and C643 cells in the control and apatinib groups are shown in the upper panel, and the number of migrating/invading cells and relative cell viability values are presented in the lower panels. The data are presented as the mean ± S.D. ***P < 0.001. (b). Expression levels of N-cad, Slug, snail1 and MMP-9 were determined by western blot after treatment with apatinib. GAPDH was used as an internal control.

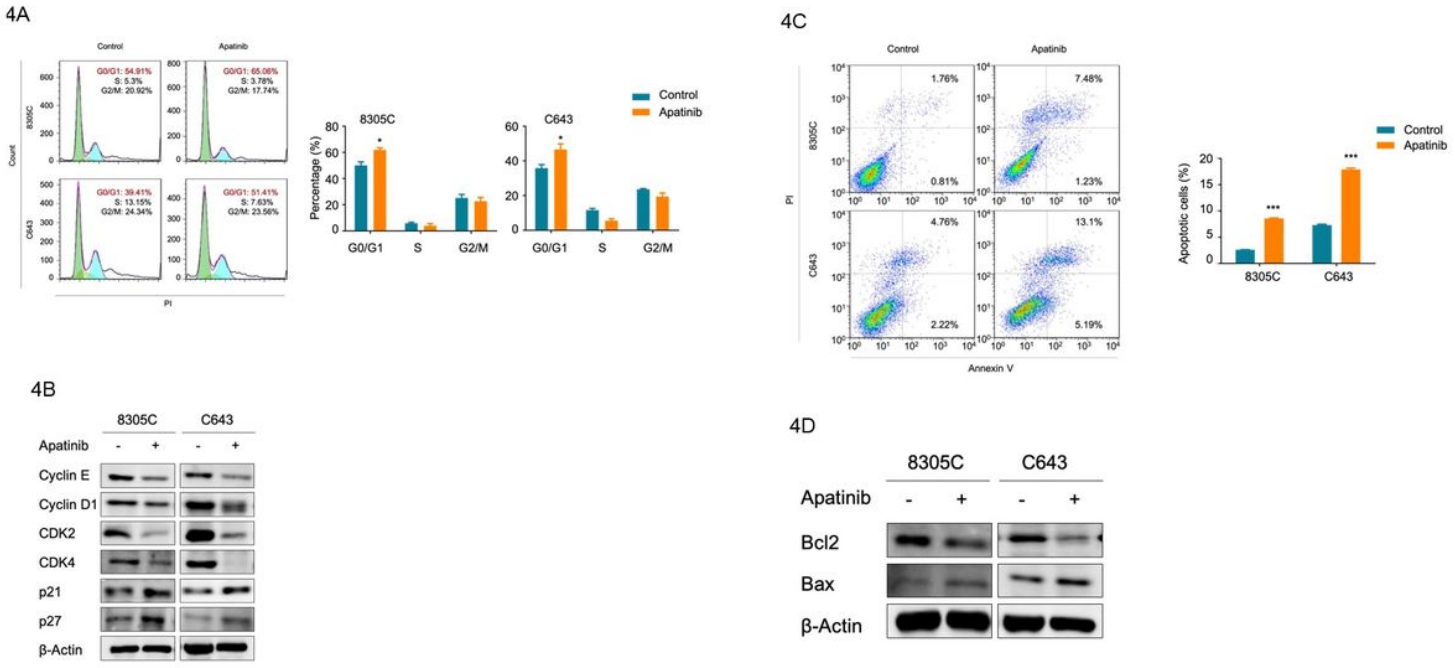

Figure 4

Induction of cell cycle arrest and apoptosis by apatinib in TC cells. (a). Representative flow cytometry profiles are shown in the left panels, and the percentage of cells in each cell cycle phase is presented in the right panels. * P <0.05. (b). The expression of cell cycle-associated proteins, including cyclin-E, cyclin-D1, CDK2, CDK4, p21 and p27, was analyzed by western blot. β-Actin was used as an internal control. (c). Representative flow cytometry profiles of 8505C and C643 cells. The percentage of apoptotic cells is presented in the right panels. *** P <0.001. (d). The expression of apoptosis-associated proteins, Bcl2 and Bax, was analyzed by western blot. β-Actin was used as an internal control.

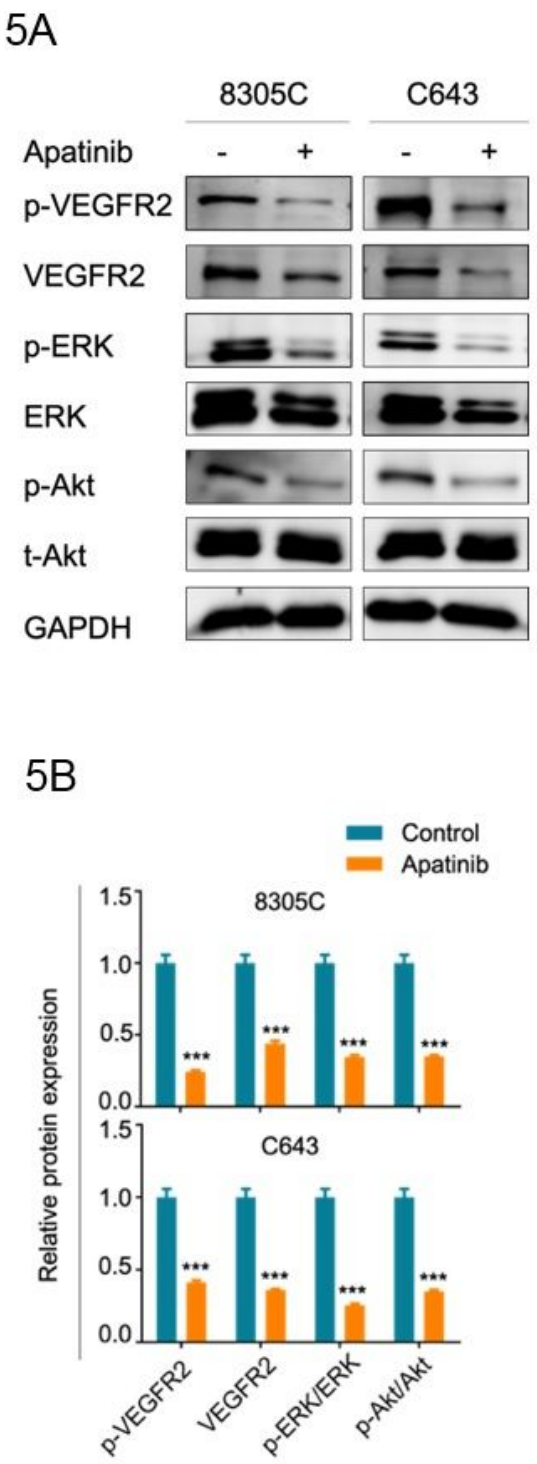

Figure 5

Effect of apatinib on members of the MAPK and PI3K-Akt signaling pathways. (a). The expression levels of p-VEGFR2, VEGFR2, p-ERK, ERK, p-Akt and t-Akt in 8305C and C643 cells were analyzed by western blot. GAPDH was used as an internal control. (b). Relative protein expression levels of p-VEGFR2, VEGFR2, p-ERK/ERK, and p-Akt/Akt in 8305C and C643 cells. The results are presented as the mean ± S.D. ***P<0.001.

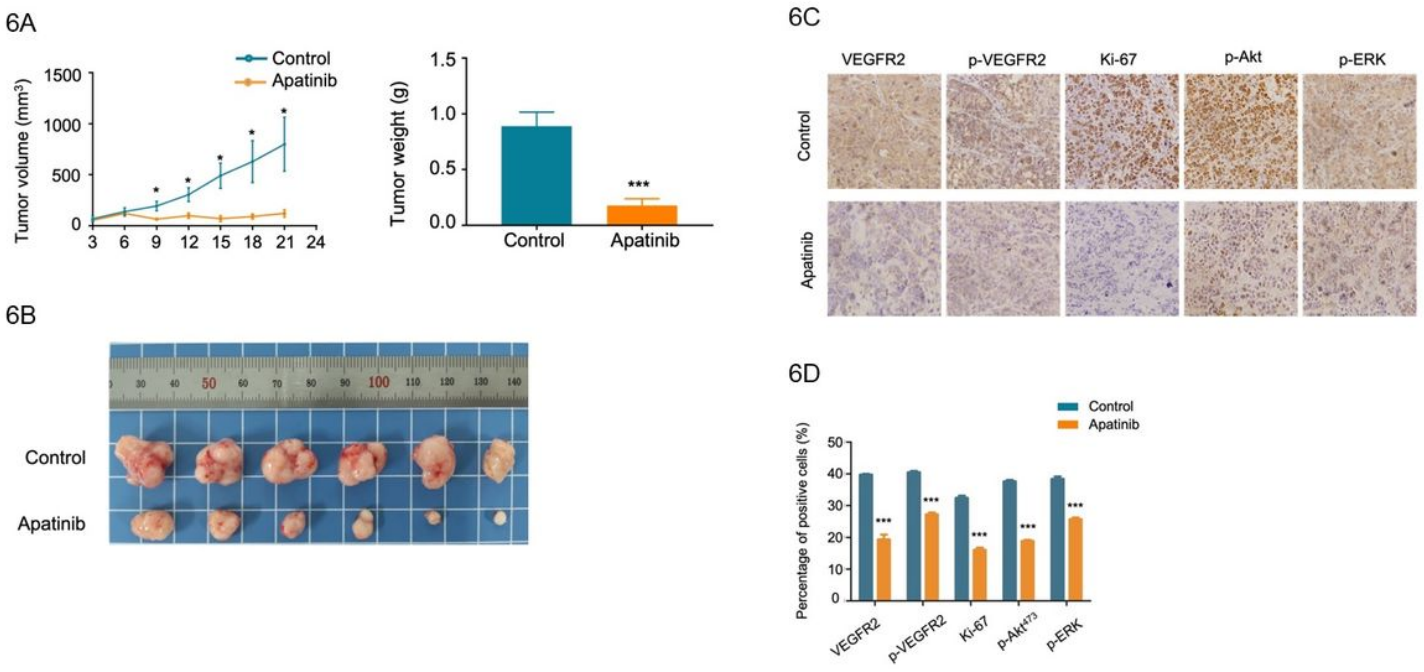

Figure 6

Apatinib inhibited tumor growth in mice with TC xenografts. (a). Tumor growth curves and tumor weights for the control and apatinib groups. (b). Representative images of xenograft tumors from the control and apatinib groups. Tumor volume was calculated every 3 days. The results are presented as the mean ± S.D. *P<0.05. (c). Representative immunohistochemistry images of VEGFR2, p-VEGFR2, Ki-67, p-Akt and p-ERK staining in the xenograft tumors. (d). The percentages of cells positive for VEGFR2, p-VEGFR2, Ki-67, p-Akt and p-ERK expression in xenograft tumors. The results are presented as the mean ± S.D. ***P 0.001.